Biochimica et Biophysica Acta 1838 (2014) 465–473

Contents lists available at ScienceDirect

Biochimica et Biophysica Acta

journal homepage: www.elsevier.com/locate/bbamem

Effects of azole treatments on the physical properties of *Candida albicans* plasma membrane: A spin probe EPR study

Cristina Sgherri [a], Amalia Porta [b], Sabrina Castellano [b], Calogero Pinzino [c], Mike F. Quartacci [a], Lucia Calucci [c,*]

[a] Dipartimento di Scienze Agrarie, Alimentari ed Agro-ambientali, Università di Pisa, via del Borghetto 80, 56124 Pisa, Italy
[b] Dipartimento di Farmacia, Università di Salerno, via Giovanni Paolo II, 84084 Fisciano, Salerno, Italy
[c] Istituto di Chimica dei Composti OrganoMetallici, Consiglio Nazionale delle Ricerche - CNR, Area della Ricerca di Pisa, via G. Moruzzi 1, 56124 Pisa, Italy

ARTICLE INFO

Article history:
Received 24 June 2013
Received in revised form 18 October 2013
Accepted 22 October 2013
Available online 31 October 2013

Keywords:
Candida albicans
Membrane fluidity
Doxyl-stearic acid
Fluconazole
Antifungal azole

ABSTRACT

EPR spectroscopy was applied to investigate the effects of the treatment of *Candida albicans* cells with fluconazole (FLC) and two newly synthesized azoles (CPA18 and CPA109), in a concentration not altering yeast morphology, on the lipid organization and dynamics of the plasma membrane. Measurements were performed in the temperature range between 0 °C and 40 °C using 5-doxyl- (5-DSA) and 16-doxyl- (16-DSA) stearic acids as spin probes. 5-DSA spectra were typical of lipids in a highly ordered environment, whereas 16-DSA spectra consisted of two comparable components, one corresponding to a fluid bulk lipid domain in the membrane and the other to highly ordered and motionally restricted lipids interacting with integral membrane proteins. A line shape analysis allowed the relative proportion and the orientational order and dynamic parameters of the spin probes in the different environments to be determined. Smaller order parameters, corresponding to a looser lipid packing, were found for the treated samples with respect to the control one in the region close to the membrane surface probed by 5-DSA. On the other hand, data on 16-DSA indicated that azole treatments hamper the formation of ordered lipid domains hosting integral proteins and/or lead to a decrease in integral protein content in the membrane. The observed effects are mainly ascribable to the inhibition of ergosterol biosynthesis by the antifungal agents, although a direct interaction of the CPA compounds with the membrane bilayer in the region close to the lipid polar head groups cannot be excluded.

1. Introduction

Serious infections caused by opportunistic fungal pathogens are increasingly common, especially in immunocompromised patients. In particular, the incidence of candidiasis has increased 5-fold in the past 10 years because of the widespread use of broad spectrum antibiotics and the more and more expanded use of immunosuppressive agents, radiotherapy and antitumoral drugs [1–3]. Azole antifungals, the major drugs used to treat pathogenic infections by *Candida albicans* [4–6], act mainly by inhibiting the activity of sterol 14α-demethylase (Erg11p/CYP51p), the key enzyme in sterol biosynthesis in yeasts and molds [7–9]. As a consequence, depletion of ergosterol and accumulation of toxic 14α-methyl-sterols occur in the plasma membrane, leading to the inhibition of fungal cell growth. Although azole antifungal agents are still considered the drugs of choice to treat most of the *Candida* infections, the resistance of *C. albicans* to most clinically used azoles, especially fluconazole (FLC, Fig. 1), is reported with increasing frequency [10,11].

In the search for novel antifungal agents endowed with broad spectrum activities and able to overcome drug resistance, we have recently presented two new azole compounds, CPA18 and CPA109 (Fig. 1) [12], acting in vitro against an FLC-sensitive and two FLC-resistant *C. albicans* strains, one with a mutation in Erg11 sequences and the other overexpressing the ABC transporter genes CDR1 and CDR2, which encode ATP-dependent efflux pumps [13]. Moreover, while FLC has only fungistatic action against *C. albicans*, the killing activity of CPA18 was remarkable and fast on azole-susceptible as well as on azole-resistant strains. Investigations aimed at ascertaining the mechanism of action of CPA azoles indicated that the binding affinities of CPA18 and CPA109 for *C. albicans* Erg11p are comparable to that of FLC. However, CPA compounds showed a superior ability in blocking germ tube formation and, differently from FLC, inhibited the polarization of sterols at the actively growing hyphal tips and increased the permeability of cells [13]. Specific alterations in the membrane lipid composition were also caused by the treatment of *C. albicans* cells with CPA compounds and FLC. As expected, all treatments resulted in a dramatic reduction in the ergosterol content, with a corresponding increase in the lanosterol one. However, a decrease of the free sterols to phospholipids (FS/PL) molar ratio was found only for the CPA

Abbreviations: 5-DSA, 5-doxylstearic acid; 16-DSA, 16-doxylstearic acid; CPA18, 1-(1-(biphenyl-4-yl)-3-(4-fluorophenyl)propan-2-yl)-1*H*-imidazole; CPA109, 1-(1-(biphenyl-4-yl)-3-(5-chlorothiophen-2-yl)propan-2-yl)-1*H*-imidazole; FLC, fluconazole; EPR, Electron Paramagnetic Resonance; MOMD, microscopically ordered macroscopically disordered; PL, phospholipid; PE, phosphatidylethanolamine; PS, phosphatidylserine; PI, phosphatidylinositol; PG, phosphatidylglycerol; PA, phosphatidic acid; FS, free sterols

* Corresponding author. Tel.: +39 050 3152517; fax: +39 050 3152555.
E-mail address: lucia.calucci@pi.iccom.cnr.it (L. Calucci).

0005-2736/$ – see front matter © 2013 Elsevier B.V. All rights reserved.
http://dx.doi.org/10.1016/j.bbamem.2013.10.015

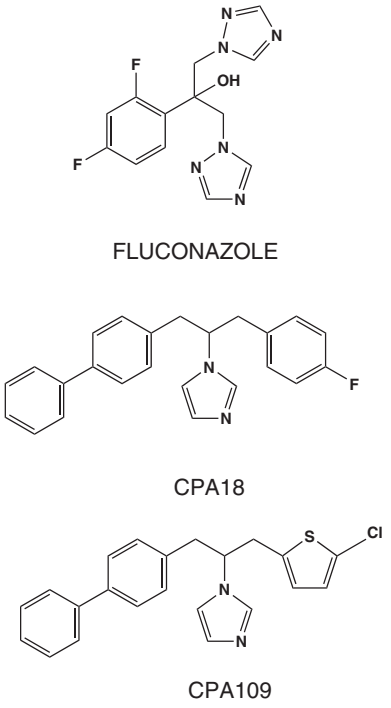

Fig. 1. Molecular structure of fluconazole (FLC), CPA18, and CPA109.

treatments. A concomitant change of PL's composition was also observed; the content of all negatively charged PLs increased, with the only exception of phosphatidylglycerol (PG) in FLC-treated cells, while that of both phosphatidylcholine (PC) and phosphatidylethanolamine (PE) decreased, the PC/PE molar ratio being reduced, especially for the CPA treatments [13].

Lipid composition and organization of plasma membrane play a multifaceted role in *C. albicans* physiology and drug susceptibility, by mediating environment sensing, nutrient uptake, drug diffusion and extrusion, virulence factor secretion, cellular morphogenesis, and cell wall biogenesis [14–17]. Indeed, the organization of plasma membrane proteins and lipids into lateral domains with different composition and degree of order was recently reported for yeasts [15,18–22]. The presence of ergosterol modulates the thickness, fluidity and permeability of the plasma membrane. Its preferential association with sphingolipids to form raft-like domains [23–26] confers membrane heterogeneity and facilitates specific functions of raft-associated proteins. In yeast, lipid rafts have been found to be implicated in protein sorting, signal transduction, secretion, endocytosis, and cell polarity [18,27–31].

The deleterious impact of altered sterol composition, and especially ergosterol depletion, in membrane packing was reported by some authors for the plasma membrane of *C. albicans* and *Saccharomyces cerevisiae* by fluorescence and EPR techniques [32–39]. Moreover, Erg mutants which possess higher levels of membrane fluidity were found to be hypersensitive to drugs [36] and membrane fluidity was shown to increase in gradually fluconazole adapted strains [38].

All this considered, an investigation of the effects induced on the membrane physical state by the treatment of *C. albicans* cells by different azole antifungals is valuable for the deeper understanding of the mechanism of action and the difference in antimicotic activity of these agents as well as for the development of novel therapeutic approaches. To this aim, in the present work we applied spin probing EPR spectroscopy, a very sensitive technique for obtaining information on the lipid organization and dynamics in natural and model membranes [40–46], to membrane vesicles isolated from *C. albicans* cells grown for about 12 h in the exponential phase in a medium containing or not CPA18, CPA109, or FLC. To obtain membrane vesicles, the concentration used for the azole compounds was able to induce only a moderate reduction in fungal growth compared to the control, without any alteration of yeast morphology. Two spin probes were used, 5- and 16-doxyl-stearic acids (5-DSA and 16-DSA in Fig. 2), to investigate the bilayer properties close to the polar head groups and to the membrane core, respectively. Indeed, although there is a distribution in the position of the nitroxide moiety due to the presence of vertical fluctuations of the spin probe alkyl chain, the mean value of the distribution, which may be considered accurate within 1.5–3.4 Å, certainly shifts toward the center of the bilayer passing from 5- to 16-DSA [45]. In particular, 5-DSA gives information on the average order and dynamic properties of lipids close to the membrane surface and has already been used to investigate *C. albicans* plasma membranes [47–49]. On the other hand, 16-DSA, as other lipids that are spin-labeled close to the methyl end of the acyl chains, can be exploited to distinguish and characterize lipid domains directly interacting with the integral membrane proteins and fluid bilayer regions of the membrane [42–44,46]. A spectral line shape analysis was performed in order to obtain quantitative information on the organization of the plasma membrane in domains with different degree of lipid orientational order and dynamics, and on the effects of the antifungal treatments on these properties.

2. Materials and methods

2.1. Materials

CPA18 and CPA109 were prepared according to the previously reported procedures [12].

FLC, 5-DSA and 16-DSA spin probes were purchased from Sigma-Aldrich.

2.2. Isolation of plasma membranes

An overnight culture of *Candida* SC5314 was diluted to 1.5×10^4 cells/mL in yeast nitrogen base (YNB) containing 0.05 mg/L of CPA109, CPA18, FLC or only vehicle (as control) and incubated with shaking (160 rpm) at 28 °C for 10–14 h (exponential phase).

Spheroplasts from *Candida* SC5314 were prepared following a slight modification of the procedure reported by Li and Cutler [50]. Exponential-phase yeast cells were washed with 50 mM Tris/HCl, pH 7.5, containing 0.25 M sucrose and 10 mM EDTA (disodium salt). Cells were pelleted by centrifugation at 1500 *g* for 10 min and suspended with the same buffer (2 mL/g wet weight) containing Zymolase 20T at 80 units per g wet weight of yeast cells. After incubation at 36 °C for 60 min under continuous agitation, cells were pelleted centrifuging at 1500 *g* for 30 min. Cells were osmotically shocked by suspension in 50 mM Tris/HCl, pH 7.5, and cell debris were removed by centrifugation at 3000 *g* for 10 min. The mitochondrial pellet was eliminated by centrifugation at 15,000 *g* for 20 min and the microsomal fraction was collected after centrifugation at 6500 *g* for 30 min [51].

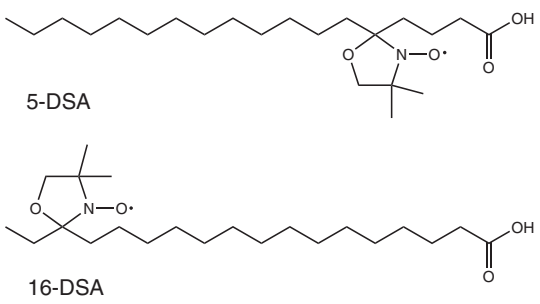

Fig. 2. Molecular structure of 5-DSA and 16-DSA.

The microsomal pellet was resuspended in 2 mL of a buffer containing 5 mM potassium phosphate, pH 7.8, 0.25 M sucrose and 3 mM KCl. The plasma membrane was isolated by loading the microsomal suspension (1 g) onto an aqueous two phase polymer system to give a final composition of 6.5% (w/w) Dextran T500, 6.5% (w/w) polyethylene glycol, 5 mM potassium phosphate (pH 7.8), 0.25 M sucrose, and 3 mM KCl. The plasma membrane was further purified using a two-step batch procedure. The resulting upper phase was diluted four-fold with 50 mM Tris/HCl, pH 7.5, containing 0.25 M sucrose, and centrifuged at 100,000 *g* for 30 min. The resultant pellet was resuspended in the same buffer containing 30% ethylene glycol and stored at −80 °C. All steps of the isolation procedure were carried out at 4 °C.

In order to check the purity of the plasma membrane, the activity of the vanadate-sensitive ATPase as a marker enzyme was determined. Cytochrome c oxidase, NADH cytochrome c reductase, and NO_3^--sensitive ATPase activities were used as markers of mitochondria, endoplasmic reticulum, and tonoplast, respectively. Tests with the markers showed that, as a mean value of the isolations performed, ATPase specific activity was 66% higher in the plasma membrane than in the microsomal fraction; vanadate inhibited ATPase activity by 88% in the plasma membrane fractions and by 35% in the microsomal ones. The addition of KNO_3 negligibly reduced ATPase activity in the plasma membrane fractions (6% inhibition). The specific activities of marker enzymes such as cytochrome c oxidase and NADH cytochrome c reductase in the upper phase of both plasma membrane were 4 and 8% of those determined in the lower phase, respectively.

2.3. Spin labeling

Plasma membrane vesicles were suspended in 500 μL of 50 mM Tris/HCl, pH 7.5, and some aliquots were used to detect protein amounts following a previously reported procedure [52]. Spin labeling was performed incubating overnight at room temperature aliquots of membranes containing 300 μg protein with 1.5 μmol of 5-DSA or 16-DSA. Membranes were then washed three times in 50 mM Tris/HCl, pH 7.5, and centrifuged at 100,000 *g* for 15 min. Free spin probes were not detected in the supernatant following the third washing.

2.4. EPR measurements

For EPR measurements, each sample was transferred into a 100 μL capillary tube which was sealed at both ends, inserted into a quartz sample holder, and put in the microwave cavity of the spectrometer. EPR spectra were recorded using a Varian (Palo Alto, CA, USA) E112 spectrometer operating at X band. Spectra were recorded every 5 °C in the 0–40 °C interval on temperature raising, waiting 10 min for equilibrating the temperature. For each spectrum a microwave power of 2 mW and a modulation amplitude of 1.0 Gauss were employed.

The rigid limit spectra were recorded at −150 °C using a microwave power of 2 mW and a modulation amplitude of 2.0 Gauss.

2.5. Line shape analysis

The EPR spectral line shapes were analyzed using the non-linear-least-squares fitting program developed by Budil et al. [53], based on the Freed's theory of slow motion EPR [54,55]. The microscopically ordered and macroscopically disordered (MOMD) model proposed by Meirovitch et al. [56,57] was used to reproduce the characteristics of the dynamic structure of the membrane samples, where lipid molecules are locally oriented by the bilayer structure, but globally the lipid bilayer segments are distributed randomly. The motion of the nitroxide moiety attached to the Cn position of the stearic acid chain (Fig. 2) was treated as Brownian axial diffusion and described by two diffusion coefficients: $R_{\|}$, representing the rotation of the spin probe about its long axis, and $R_{\perp}$, governing the wobbling of the long axis within a cone. The order parameter, S, is a measure of the angular extent of the rotational diffusion of the principal nitroxide axis system with respect to the membrane director, which is perpendicular to the bilayer plane. The larger the S value, the more restricted is the motion, which usually means that laterally the lipid molecules surrounding the nitroxide are packed more tightly.

Our spectra were insensitive to $R_{\|}$, as already pointed out for EPR spectra of macroscopically unaligned bilayers by other authors [58,59]; therefore, in all the calculations $R_{\|}$ was kept fixed at a value of 10^8–10^9 s^{-1}. Each spectrum was fitted by the sum of two sub-spectra, each characterized by a population and a couple of $R_{\perp}$ and S fit parameters. In the calculations the following values were employed for the principal components of the **g** and hyperfine interaction (**A**) tensors: $g_{xx} = 2.0088$, $g_{yy} = 2.0061$, $g_{zz} = 2.0027$; $A_{xx} = A_{yy} = 5.5$ Gauss, $A_{zz} = 34.4$ Gauss for the **a** component of 5-DSA and $A_{xx} = A_{yy} = 4.9$ Gauss, $A_{zz} = 32.6$ Gauss for the **a** and **b** components of 16-DSA. These values were determined from the rigid limit spectra of the different samples, for which they were found to be equal within 0.2 Gauss. For the **b** component of the 5-DSA spectra the same principal components of the **g** tensor were used but with $A_{xx} = A_{yy} = 5.1$ Gauss and $A_{zz} = 33.4$ Gauss. A Lorentzian line width tensor (w_{xx}, w_{yy}, w_{zz}) was employed to take into account inhomogeneous broadening [53] with $w_{xx} = w_{yy} = w_{zz}$. Values of w_{ii} of 4.6 and 1.1 Gauss were used for the **a** and **b** components of the 5-DSA spectra, respectively. The values of w_{ii} used for calculating 16-DSA spectra were of 4.6 and 2.4 Gauss for the **a** and **b** components, respectively, except for the 16DSA-FLC sample, for which the w_{ii} values of the **b** component were taken to be 1.1 Gauss. 30 orientations were considered in all calculations.

3. Results and discussion

3.1. EPR spectra of C. albicans plasma membrane: identification of lipid domains

X-band EPR spectra in membranes isolated from *C. albicans* cells, untreated (sample nDSA-control, with n = 5 and 16) and treated with CPA18, CPA109, or FLC (samples nDSA-CPA18, nDSA-CPA109, and nDSA-FLC, respectively, with n = 5 and 16), were recorded every 5 °C in the 0 °C to 40 °C temperature range using 5-DSA and 16-DSA spin probes; a representative selection is shown in Figs. 3 and 4. As it can be observed, the spectra show up to three distinguishable components, with characteristic features indicated with **a**, **b**, and **c** in Figs. 3 and 4, corresponding to spin probes in different environments. In particular, a minor component (**c**, indicated by arrows in Figs. 3A and 4D), with a line shape typical of spin probes undergoing fast isotropic motion, was observed in some cases. On the basis of the isotropic hyperfine coupling constant (15.6 Gauss), which was almost equal to that of the spin probes in buffer solution, and considering that the line shape does not vary much with temperature, this component was attributed to a negligible fraction of spin probe molecules not incorporated in the membrane bilayer, which remains free in the surrounding buffer. Therefore, this component was not considered in the line shape analysis and in the discussion reported below. The main spectral components were due to spin probes inserted in the membrane bilayer. In particular, the 5-DSA spectra (Fig. 3) were essentially ascribable to strongly immobilized spin probes (component **a**) with only a minor contribution from weakly immobilized ones (component **b**). On the other hand, the spectra recorded using the 16-DSA spin probe (Fig. 4) showed a strongly (**a**) and a weakly (**b**) immobilized components with comparable relative intensities. By increasing the temperature, a line shape evolution characteristic of a general increase in mobility of both spin probes inside the membrane bilayer was observed for all the samples; indeed, the outer hyperfine splitting of the **a** component and the line widths of the **b** component decreased on heating (Figs. 3 and 4). In particular, as shown in Fig. 5, the outer hyperfine splittings ($2A_{zz}$) of the **a** component in the 5-DSA spectra ranged between 66.0 ± 0.3 Gauss and 57.8 ± 0.3 Gauss on going from 0 °C to 40 °C, while the distances between the

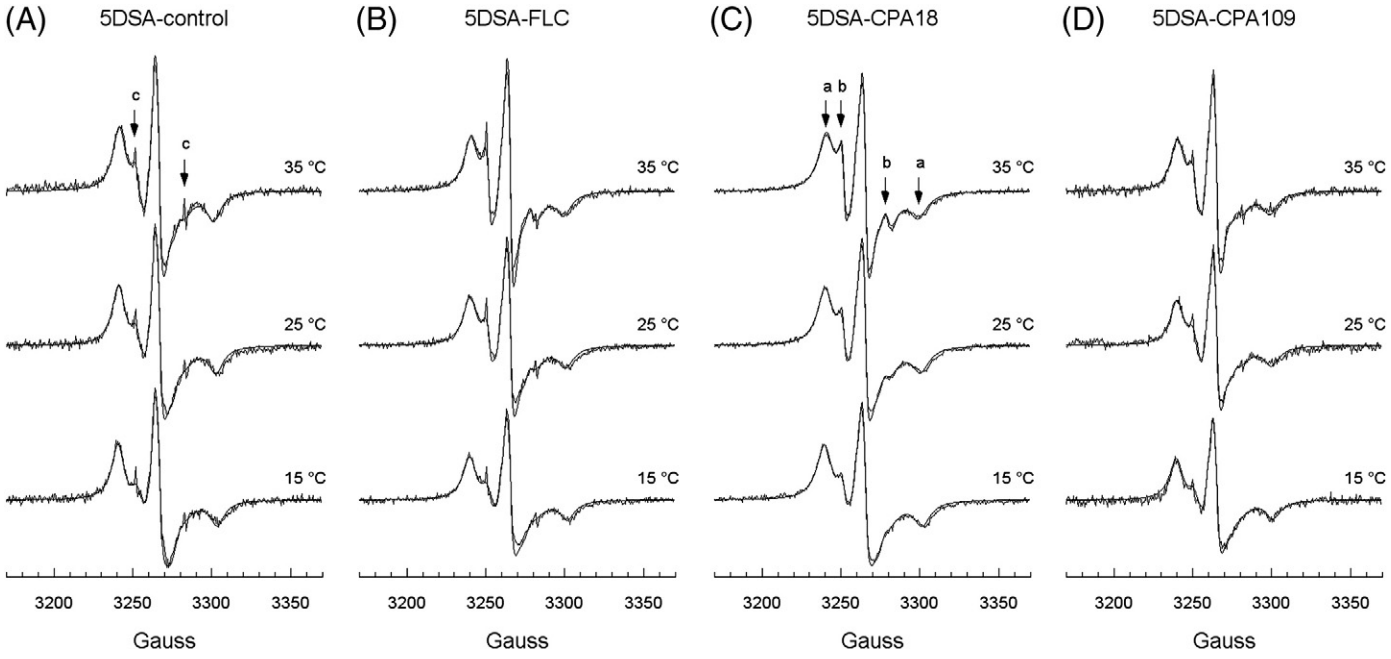

Fig. 3. Experimental and calculated EPR spectra of samples 5DSA-control (A), 5DSA-FLC (B), 5DSA-CPA18 (C) and 5DSA-CPA109 (D) at the indicated temperatures.

outer lines of the **b** component were of 28.0 ± 0.3 Gauss at all the investigated temperatures. The maximum splittings of the **a** and **b** components in the spectra of 16-DSA were more difficult to determine due to the superposition of the two components; however, values ranging from 62 ± 1 Gauss (at 0 °C) to 51 ± 2 Gauss (at 40 °C) could be measured for the **a** component in the different samples, whereas for the **b** component the maximum splitting was of 28.3 ± 0.3 Gauss for all the samples at all the temperatures. Moreover, the outer hyperfine splittings ($2A_{zz}$) determined from the rigid limit spectra of 5-DSA and 16-DSA in the different samples were of 68.8 ± 0.3 Gauss and 65.2 ± 0.3 Gauss, respectively, indicating that, as expected, there is a decreasing gradient of hydrophobicity on going from the membrane interior to the region close to the surface [60–62]. The isotropic hyperfine splitting determined for the **b** component of the 5-DSA spectra (14 Gauss) is much lower than that determined from the hyperfine tensor components (15.1 Gauss). On the basis of this finding and of the almost isotropic line shape, the **b** component can be ascribed to a minor fraction of disordered lipids present in the samples [45,63–65].

In protein containing membranes, the **a** and **b** spectral components observed for 16-DSA can be ascribed to lipids interacting with intramembraneous proteins and to bulk lipids, respectively [43–46]. In *C. albicans* plasma membrane, where many integral proteins are preferentially associated with highly ordered lipid domains formed by ergosterol and sphingolipids segregating from a more disordered phase

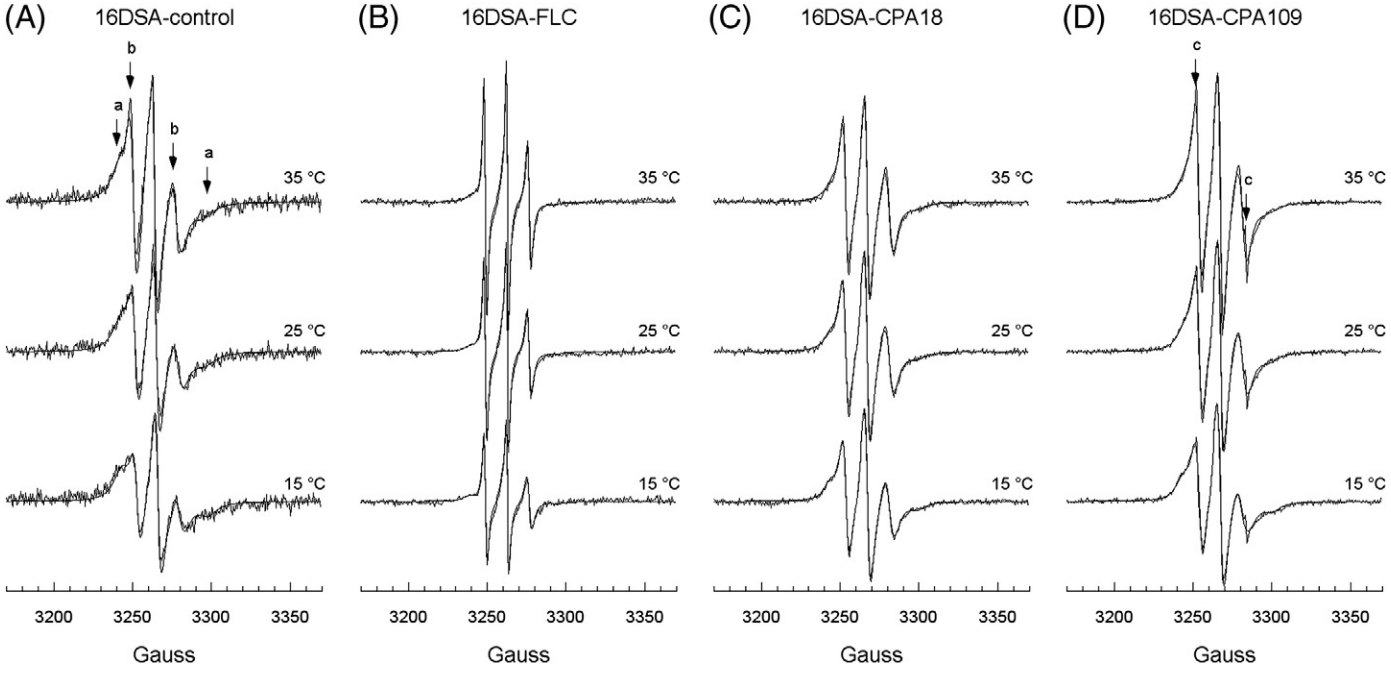

Fig. 4. Experimental and calculated EPR spectra of samples 16DSA-control (A), 16DSA-FLC (B), 16DSA-CPA18 (C) and 16DSA-CPA109 (D) at the indicated temperatures.

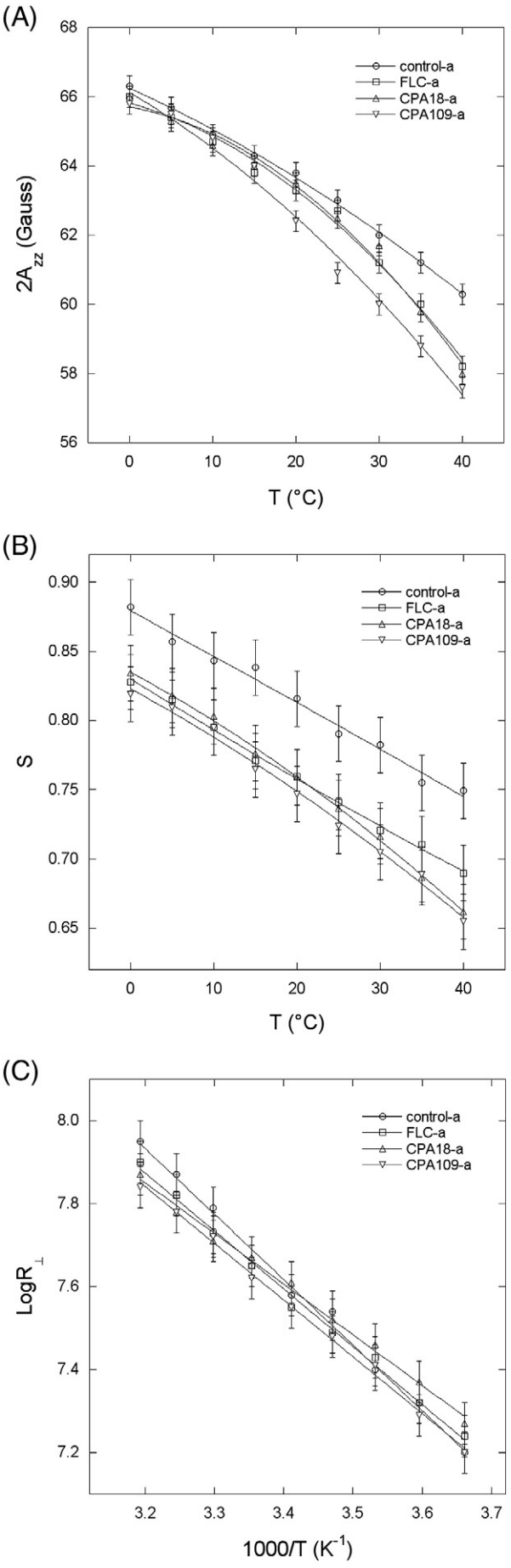

containing glycerophospholipids [15,18,20,21], the **a** component of the 16-DSA spectra could therefore arise from spin probes in protein–lipid domains. Indeed, in the time frame for X-band EPR (100 ps to 10 ns), the spectra of 16-DSA are sharp in disordered lipid domains and broad in ordered lipid domains around integral membrane proteins (boundary lipids) or trapped between protein molecules (trapped lipids). On the other hand, both bulk and protein-interacting lipid components show broad sub-spectra for 5-DSA, which cannot be discriminated in X-band spectra; in the 5-DSA spectra of our samples they both contribute to the **a** component.

In order to determine the relative amount of spin probes in the different environments and to characterize their degree of orientational order and dynamics, we performed a nonlinear least squares fitting of the experimental spectra based on the theory of slow motion EPR [53]. As reported in Section 2.5, we considered an MOMD model [56,57] for the description of the lipid bilayers and an axial Brownian rotational diffusion model for the spin probe motion. Since the **a** and **b** components of the 5-DSA and 16-DSA spectra are distinguishable at all the investigated temperatures, we considered the translational diffusion of the spin probes between the different domains slow and we fitted the spectra as the superposition of two sub-spectra corresponding to the **a** and **b** components (see Fig. 6), each calculated optimizing the values of the rotational diffusion coefficient $R_{\perp}$ and the order parameter S (see Section 2.5) and of the relative population. However, as pointed out by Ge and Freed [58], the X-band EPR spectra of unaligned lipid bilayer samples have limited resolution, the superposition of spectra from all bilayer director orientations giving rise to inhomogeneous broadening that tends to mask the homogeneous broadening relating to the molecular dynamics. As a result, the fitting of the spectra can be ambiguous. Here, the superposition of two spectral components could be a further source of ambiguity in the fitting. Indeed, in the case of 16-DSA spectra, a quite strong correlation was found between $R_{\perp}$ and S for the **a** component, whereas populations and $R_{\perp}$ and S values for the **b** component could be more reliably determined. For the 5-DSA spectra, being their intensity very small, the $R_{\perp}$ and S parameters of the **b** component were determined with a higher uncertainty. All this considered, populations and $R_{\perp}$ and S parameters of the **a** component could be determined without ambiguity. Adopting this strategy, the line shape of all the recorded spectra was satisfactorily reproduced, as exemplified in Figs. 3 and 4, and ordering and dynamic parameters and weights for the component spectra could be determined, although with a different degree of uncertainty. Nevertheless, in all cases they could be used to interpret trends related to temperature change and sample treatment.

For the 5-DSA spectra, the **a** component accounted for 97–99%, 92–98%, 94–99%, and 95–99% of the total spectral intensity for samples 5DSA-control, 5DSA-FLC, 5DSA-CPA18, and 5DSA-CPA109, respectively, the contribution decreasing with increasing the temperature. The $R_{\perp}$ and S values, reported in Fig. 5, were typical of lipids with relatively high mobility and high degree of orientational order. In all cases, the $R_{\perp}$ and S values regularly increased and decreased with increasing the temperature, respectively; in particular, the trends of $R_{\perp}$ vs T could be well reproduced by the Arrhenius equation giving activation energy values of 31 ± 2, 28 ± 2, 23 ± 2, and 26 ± 2 kJ/mol for 5DSA-control, 5DSA-FLC, 5DSA-CPA18, and 5DSA-CPA109 samples, respectively. These values are in the order of those found for other membranes and phospholipid bilayers [66,67], the slightly lower values found for the treated samples indicating a lower sensitivity of these systems to temperature changes with respect to the control. The minor **b** component in the 5-DSA spectra of the different samples was characterized

Fig. 5. (A) $2A_{zz}$ values measured for the **a** component from the spectra of 5-DSA-control, 5-DSA-FLC, 5DSA-CPA18, and 5DSA-CPA109 samples. (B) Orientational order parameter (S) vs T of the **a** spectral component of 5-DSA in the indicated samples; lines are drawn to guide the eyes. (C) $LogR_{\perp}$ vs 1000/T of the **a** spectral component of 5-DSA in the indicated samples; lines represent fits to the Arrhenius equation.

by $R_\perp$ and S values of $(1.6 \pm 0.2) \times 10^8\ s^{-1}$ and 0.15 ± 0.05, respectively, these values being compatible with an environment with quite high mobility and almost isotropic ordering. For the 16-DSA spectra, the **a** component accounted for 78–82%, 45–51%, 52–61%, and 55–66% of the total spectral intensity for samples 16DSA-control, 16DSA-FLC, 16DSA-CPA18, and 16DSA-CPA109, respectively, the contribution decreasing with increasing the temperature. This component was characterized by quite high orientational order and quite slow dynamics, the S values ranging from 0.83 ± 0.03 to 0.45 ± 0.05 (Fig. 7) and $R_\perp$ values from $(3.2 \pm 0.4) \times 10^7$ to $(1.0 \pm 0.1) \times 10^8\ s^{-1}$, on raising the temperature from 0 °C to 40 °C. On the other hand, for the fluid and almost isotropic **b** component of 16-DSA spectra, S values ranging from 0.10 to 0.15 were determined for all the samples except for 16DSA-FLC for which S was 0.05 ± 0.03. The $R_\perp$ values obtained for the **b** component ranged from $(1.0 \pm 0.1) \times 10^8$ to $(5.0 \pm 0.2) \times 10^8\ s^{-1}$ (Fig. 7) and their trends vs T could be well reproduced by the Arrhenius equation with activation energies of 25 ± 2, 22 ± 2, 30 ± 2, and 20 ± 2 kJ/mol for 16DSA-control, 16DSA-FLC, 16DSA-CPA18, and 16DSA-CPA109 samples, respectively. These activation energy values are on the order of those determined for 5-DSA, and no clear trend is found as a function of the azole treatment.

3.2. Effects of the azole treatments on plasma membrane properties

The EPR spectra of 5-DSA and 16-DSA recorded on the different plasma membrane samples, although with common general features, showed significant differences which can be related to the effect of the azole treatments on *C. albicans* cells. In particular, for the membrane region close to the polar head groups, explored by the 5-DSA spin probe, a higher fluidity was found for treated samples as indicated by the lower values of the outer hyperfine splitting (Fig. 5A) and by the lower order parameter values determined from the fitting of the main spectral component (Fig. 5B). Therefore, the treatment of *C. albicans* cells with the azole antifungal agents here investigated seems to loosen the packing of the membrane lipids close to the polar head group region. Moreover, a slightly higher contribution of the **b** component to the spectral intensity of the 5-DSA spectra was found for the treated samples with respect to the control one; indeed the **b** component accounted for less than 3% of the spectral intensity for 5DSA-control and for less than 8%, 6% and 5% for 5DSA-FLC, 5DSA-CPA18, and 5DSA-CPA109, respectively. This could be seen as an increase in content of very fluid lipid domains in the membrane induced by the treatments.

EPR spectroscopy with the 5-DSA spin probe was also applied to investigate the fluidity of plasma membrane in *S. cerevisiae* strains [35]; lower order parameters were found for strains producing lower levels of ergosterol. An increased fluidity of the plasma membrane interfacial region was also found by time-resolved fluorescence spectroscopy for *S. cerevisiae* in which the ergosterol content was decreased by an FLC treatment [33] or using mutants defective in the late stage of ergosterol biosynthesis [32,34]. As far as *C. albicans* is concerned, higher fluidity of the plasma membrane was also found for FLC resistant strains depleted in ergosterol [36–39]. In all cases the observed findings were ascribed to the deleterious impact of altered sterols, and in particular of ergosterol depletion, on membrane packing. Correspondingly, the dramatic decrease in ergosterol content previously found for *C. albicans* treated with the azoles here investigated [13] can account for the looser packing in the region close to the lipid head groups. The slightly higher fluidity found for CPA with respect to FLC treatments could be associated to the lower free sterol to phospholipid ratio. However, the direct interaction with CPA compounds could also contribute to change the plasma membrane packing. Indeed, a recent study on the effect of CPA18 and FLC on the physico-chemical properties of DOPC and DOPC/ergosterol bilayers, performed by EPR spectroscopy using 5-DSA and 16-DSA as spin probes, clearly indicated that, both in the presence and in the absence of ergosterol, CPA18 loosens the phospholipid packing of DOPC in the region close to the polar head groups and only slightly affects the bilayer core, whereas FLC does not alter the bilayer organization and dynamics [68]. Since phosphatidylcholine and ergosterol are the main phospholipid and sterol components, respectively, of the *C. albicans* plasma membrane, in which unsaturated phospholipids

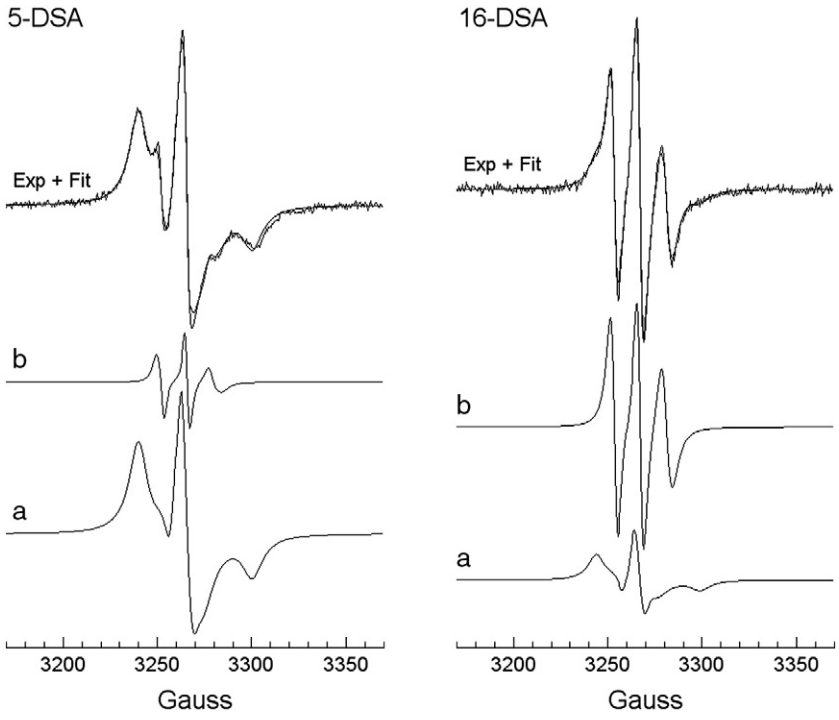

Fig. 6. Left: EPR spectrum recorded on the 5DSA-CPA18 sample at 25 °C; upper spectrum: experimental spectrum and fit; middle and lower spectra: calculated spectra of the **b** and **a** components. Right: EPR spectrum recorded on the 16DSA-CPA18 sample at 25 °C; upper spectrum: experimental spectrum and fit; middle and lower spectra: calculated spectra of the **b** and **a** components.

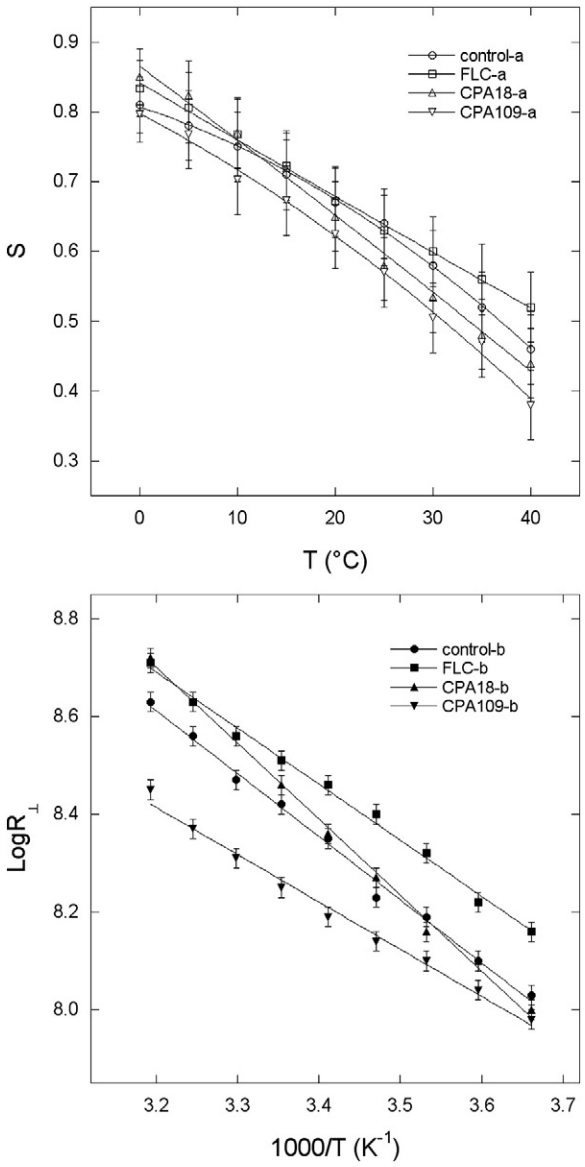

Fig. 7. Top: orientational order parameter (S) vs T of the **a** spectral component of 16-DSA in the indicated samples; lines are drawn to guide the eyes. Bottom: $LogR_{\perp}$ vs 1000/T of the **b** spectral component of 16-DSA in the indicated samples; lines represent fits to the Arrhenius equation.

constitute a considerable fraction of total phospholipids [16,69–72], the direct interactions of the azole compounds observed in the model bilayers can be considered valid also in the case of the *C. albicans* plasma membrane.

The 16-DSA spin probe allowed the effects of the azole treatments to be investigated close to the core of the plasma membrane bilayer, giving information on lipid organization and dynamics as influenced by the interactions of lipids with integral proteins. We found that, after the azole treatments, the amount of spin probes in lipid–protein domains is markedly decreased, the **a** component of the 16-DSA spectra accounting for ~80% of the spectral intensity for the control sample but for ~50%, ~55%, and ~60% for samples treated with FLC, CPA18 and CPA109, respectively. On the other hand, no significant variations of the order parameter (S) and diffusion coefficient ($R_{\perp}$) values were found for this spectral component among the different samples, indicating that the azole treatments do not markedly alter the physical state of these domains. As far as the bulk lipid domain is concerned (spectral component **b**), very low S values were found for all the samples, although no orientational order of lipids was found only for the sample treated with FLC. With respect to the control sample, the $R_{\perp}$ values were higher for the CPA18 and FLC treated samples and lower for the CPA109 treated sample (Fig. 7).

An analysis of the findings on 16-DSA to obtain detailed quantitative information on the organization of the plasma membrane is hampered, on one hand, by the high structural complexity of the membrane and, on the other hand, by the lack of knowledge of important parameters such as the stoichiometry of the protein-associated lipids, a quantity that is related to the intramembraneous structure and assembly of integral proteins, the lipid selectivity for the interaction with different membrane proteins, which depends on the nature of both specific lipids and proteins but also on the milieu properties [42–44,46], and the partition coefficient of the spin probe in the different explored domains. Nevertheless, our findings can be considered as a strong indication that the treatment of *C. albicans* cells with all the azole antifungals tested results in an alteration of the whole plasma membrane structure concerning not only lipids but also proteins. On the basis of the obtained data, a decrease in the ratio between integral proteins and lipids, a different organization of lipids to host integral proteins and/or a different structural arrangement of integral proteins in domains with different lipid compositions can be inferred. Considering the role of ergosterol in the organization of the yeast plasma membrane, it seems reasonable that the ergosterol depletion by azole antifungals would result in a decreased formation of highly ordered lipid domains specifically associated to integral proteins. To this regard, it is worth mentioning the presence in *C. albicans* lipid rafts of a series of proteins involved in lipid metabolism and multidrug efflux, such as: Erg11p and Scs7p, involved in the lipid metabolism of major raft components [73], Rta2p, a translocase that moves sphingolipid log chain bases from the inside to the outside membrane [74], and the ATP-binding cassette (ABC) multidrug transporter CaCdr1p [31].

4. Conclusions

The application of spin probing EPR spectroscopy allowed the changes in *C. albicans* membrane organization induced by the treatment of cells in the exponential phase with three azole antifungals (CPA18, CPA109, and FLC) to be highlighted. In particular, orientational order parameters, rotational diffusion rates, and populations were determined for the discernible domains, characterized by different structural and dynamic properties, by performing an analysis of the line shape of 5-DSA and 16-DSA spin probe spectra recorded at different temperatures. It is worth noticing that, although 5-DSA has already been used to probe the *C. albicans* membrane close to the lipid polar heads, to the best of our knowledge this is the first report on the use of a spin probe (here 16-DSA) to investigate the core of the plasma membrane bilayers in *C. albicans*.

Data obtained for 5-DSA clearly indicate that, regardless of the antifungal agent used, the treatment of the *C. albicans* cells results in an increase of the membrane fluidity in proximity of the membrane surface, which can be ascribed to a decrease in ergosterol content, most probably accompanied by a direct interaction with the phospholipids in the case of CPA18 and CPA109 compounds. On the other hand, the 16-DSA results point to a definite decrease in the amount of highly ordered lipids in domains hosting intramembraneous proteins, which can be associated with the depletion of ergosterol induced by the treatment with the azole compounds.

In conclusion, treatment of *C. albicans* cells with azole antifungals, even in concentrations not able to alter yeast morphology, triggers off deep alterations in membrane organization.

Funding

This work was supported by grants from Ministero dell'Università e della Ricerca Scientifica e Tecnologica - PRIN 2008 (20088L3BP3 to L.C., S.C. and A.P.).

References

[1] M. Bassetti, F. Ansaldi, L. Nicolini, E. Malfatto, M.P. Molinari, M. Mussap, B. Rebesco, F. Bobbio Pallavicini, G. Icardi, C. Viscoli, Incidence of candidaemia and relationship with fluconazole use in an intensive care unit, J. Antimicrob. Chemother. 64 (2009) 625–629.

[2] A. Gafter-Gvili, L. Vidal, E. Goldberg, L. Leibovici, M. Paul, Treatment of invasive Candidal infections: systematic review and meta-analysis, Mayo Clin. Proc. 83 (2008) 1011–1021.

[3] M.A. Pfaller, D.J. Diekema, Epidemiology of invasive candidiasis: a persistent public health problem, Clin. Microbiol. Rev. 20 (2007) 133–163.

[4] R.A. Fromtling, Overview of medically important antifungal azole derivatives, Clin. Microbiol. Rev. 1 (1988) 187–217.

[5] D.J. Sheenan, C.A. Hitchcock, Current and emerging azole antifungal agents, Clin. Microbiol. Rev. 12 (1999) 40–79.

[6] P.G. Pappas, C.A. Kauffman, D. Andes, D.K. Benjamin Jr., T.F. Calandra, J.E. Edwards Jr., S.G. Filler, J.F. Fisher, B.-J. Kullberg, L. Ostrosky Zeichner, A.C. Reboli, J.H. Rex, T.J. Walsh, J.D. Sobe, Clinical practice guidelines for the management of candidiasis: 2009 update by the Infectious Diseases Society of America, Clin. Infect. Dis. 48 (2009) 503–535.

[7] F.C. Odds, A.J. Brown, N.A. Gow, Antifungal agents: mechanisms of action, Trends Microbiol. 11 (2003) 272–279.

[8] D. Lamb, D. Kelly, S. Kelly, Molecular aspects of azole antifungal action and resistance, Drug Resist. Updat. 2 (1999) 390–402.

[9] N. Strushkevich, S.A. Usanov, H.-W. Park, Structural basis of human CYP51 inhibition by antifungal azoles, J. Mol. Biol. 397 (2010) 1067–1078.

[10] T.C. White, K.A. Marr, R.A. Bowden, Clinical, cellular, and molecular factors that contribute to antifungal drug resistance, Clin. Microbiol. Rev. 11 (1998) 382–402.

[11] A. Lupetti, R. Danesi, M. Campa, M. Del Tacca, S. Kelly, Molecular basis of resistance to azole antifungals, Trends Mol. Med. 8 (2002) 76–81.

[12] S. Castellano, G. Stefancich, R. Ragno, K. Schewe, M. Santoriello, A. Caroli, R.W. Hartmann, G. Sbardella, Cyp19 (aromatase): exploring the scaffold flexibility for novel selective inhibitors, Bioorg. Med. Chem. 16 (2008) 8349–8358.

[13] E.C. Calabrese, S. Castellano, M. Santoriello, C. Sgherri, M.F. Quartacci, L. Calucci, A.G.S. Warrilow, D.C. Lamb, S.L. Kelly, C. Milite, I. Granata, G. Sbardella, G. Stefancich, B. Maresca, A. Porta, Antifungal activity of azole compounds CPA18 and CPA109 against azole-susceptible and -resistant strains of *Candida albicans*, J. Antimicrob. Chemother. 68 (2013) 1111–1119.

[14] L.M. Douglas, H.X. Wang, S. Keppler-Ross, N. Dean, J.B. Konopka, Sur7 promotes plasma membrane organization and is needed for resistance to stressful conditions and to invasive growth and virulence of *Candida albicans*, mBio 3 (2012) e00254–e.

[15] A. Oliveira-Couto, P.S. Aguilar, Eisosomes and plasma membrane organization, Mol. Genet. Genomics 287 (2012) 607–620.

[16] A. Singh, R. Prasad, Comparative lipidomics of azole sensitive and resistant clinical isolates of *Candida albicans* reveals unexpected diversity in molecular lipid imprints, PloS One 6 (2011) e19266.

[17] A. Singh, V. Yadav, R. Prasad, Comparative lipidomics in clinical isolates of *Candida albicans* reveal crosstalk between mitochondria, cell wall integrity and azole resistance, PloS One 7 (2012) e39812.

[18] V. Wachtler, M. Balasubramanian, Yeast lipid rafts?— an emerging view, Trends Cell Biol. 16 (2006) 1–4.

[19] F.J. Alvarez, L.M. Douglas, J.B. Konopka, Sterol-rich membrane domains in fungi, Eukaryot. Cell 6 (2007) 755–763.

[20] M. Operaková, J. Malinsky, W. Tanner, Plants and fungi in the era of heterogeneous plasma membranes, Plant Biol. 12 (2010) 94–98.

[21] J. Malinsky, M. Operaková, W. Tanner, The lateral compartmentation of the yeast plasma membrane, Yeast 27 (2010) 473–478.

[22] N.E. Ziółkowska, R. Christiano, T.C. Walther, Organized living: formation mechanisms and functions of plasma membrane domains in yeast, Trends Cell Biol. 22 (2011) 151–158.

[23] X. Xu, R. Bittman, G. Duportail, D. Heissler, C. Vilcheze, E. London, Effect of the structure of natural sterols and sphingolipids on the formation of ordered sphingolipid/sterol domains (rafts), J. Biol. Chem. 276 (2001) 33540–33546.

[24] A. Arora, H. Raghuraman, A. Chattopadhyay, Influence of cholesterol and ergosterol on membrane dynamics: a fluorescence approach, Biochem. Biophys. Res. Commun. 318 (2004) 920–926.

[25] Y.-W. Hsueh, K. Gilbert, C. Trandum, M. Zuckermann, J. Thewalt, The effect of ergosterol on dipalmitoylphosphatidylcholine bilayers: a deuterium NMR and calorimetric study, Biophys. J. 88 (2005) 1799–1808.

[26] J. Czub, M. Baginski, Comparative molecular dynamics study of lipid membranes containing cholesterol and ergosterol, Biophys. J. 90 (2006) 2368–2382.

[27] M. Bagnat, S. Keränen, A. Shevchenko, K. Simons, Lipid rafts function in biosynthetic delivery of proteins to the cell surface in yeast, Proc. Natl. Acad. Sci. U. S. A. 97 (2000) 3254–3259.

[28] R.C. Dickson, C. Sumanasekera, R.L. Lester, Functions and metabolism of sphingolipids in *Saccharomyces cerevisiae*, Prog. Lipid Res. 45 (2006) 447–465.

[29] X.L. Guan, C.M. Souza, H. Pichler, G. Dewhurst, O. Schaad, K. Kajiwara, H. Wakabayashi, T. Ivanova, G.A. Castillon, M. Piccolis, F. Abe, R. Loewith, K. Funato, M.R. Wenk, H. Riezman, Functional interactions between sphingolipids and sterols in biological membranes regulating cell physiology, Mol. Biol. Cell 20 (2009) 2083–2095.

[30] Y.-Q. Zhang, R. Rao, Beyond ergosterol. Linking pH to antifungal mechanisms, Virulence 1 (2010) 1–4.

[31] R. Pasrija, S.L. Panwar, R. Prasad, Multidrug transporters CaCdr1p and CaMdr1p of *Candida albicans* display different lipid specificities: both ergosterol and sphingolipids are essential for targeting of CaCdr1p to membrane rafts, Antimic. Agents Chemother. 52 (2008) 694–704.

[32] S.C. Sharma, Implication of sterol structure for membrane lipid composition, fluidity and phospholipid asymmetry in *Saccharomyces cerevisiae*, FEMS Yeast Res. 6 (2006) 1047–1051.

[33] F. Abe, K. Usui, T. Hiraki, Fluconazole modulates membrane rigidity, heterogeneity, and water penetration into the plasma membrane of *Saccharomyces cerevisiae*, Biochemistry 48 (2009) 8494–8504.

[34] F. Abe, T. Hiraki, Mechanical role of ergosterol in membrane rigidity and cycloheximide resistance in *Saccharomyces cerevisiae*, Biochim. Biophys. Acta 1788 (2009) 743–752.

[35] N.D. Lees, M.D. Kemple, R.J. Barbuch, M.A. Smith, M. Bard, Differences in membrane order parameter and antibiotic sensitivity in ergosterol-producing strains of *Saccharomyces cerevisiae*, Biochim. Biophys. Acta 776 (1984) 105–112.

[36] K. Mukhopadhyay, A. Kholi, R. Prasad, Drug susceptibilities of yeast cells are affected by membrane lipid composition, Antimic. Agents Chemother. 46 (2002) 3695–3705.

[37] K. Mukhopadhyay, T. Prasad, P. Saini, T.J. Pucadyil, A. Chattopadhyay, R. Prasad, Membrane sphingolipid–ergosterol interactions are important determinants of multidrug resistance in *Candida albicans*, Antimic. Agents Chemother. 48 (2004) 1778–1787.

[38] A. Kholi, K. Smriti, A. Mukhopadhyay, R. Rattan, Prasad, In vitro low-level resistance to azoles in *Candida albicans* is associated with changes in membrane lipid fluidity and asymmetry, Antimic. Agents Chemother. 46 (2002) 1046–1052.

[39] N.N. Mishra, T. Prasad, N. Sharma, D.K. Gupta, Membrane fluidity and lipid composition of fluconazole resistant and susceptible strains of *Candida albicans* isolated from diabetic patients, Braz. J. Microbiol. 39 (2008) 219–225.

[40] D. Marsh, Electron spin resonance: spin labels, in: E. Grell (Ed.), Membrane Spectroscopy, vol. 31, 1981, pp. 51–142.

[41] L.M. Gordon, C.C. Curtain, Electron Spin Resonance analysis of model and biological membranes, in: R.C. Aloia, C.C. Curtain, L.M. Gordon (Eds.), Methods for studying membrane fluidity, Alan R. Liss, New York, 1988, pp. 25–88.

[42] P.F. Knowles, D. Marsh, Magnetic resonance of membranes, Biochem. J. 274 (1991) 625–641.

[43] D. Marsh, L.I. Horváth, Structure, dynamics and composition of lipid–protein interface. Perspectives from spin-labelling, Biochim. Biophys. Acta 1376 (1998) 267–296.

[44] D. Marsh, Electron spin resonance in membrane research: protein–lipid interactions, Methods 46 (2008) 83–96.

[45] W.K. Subczynski, J. Widomska, J.B. Feix, Physical properties of lipid bilayers from EPR spin labelling and their influence on chemical reactions in a membrane environment, Free Radic. Biol. Med. 46 (2009) 707–718.

[46] D. Marsh, Electron spin resonance in membrane research: protein–lipid interactions from challenging beginnings to state of the art, Eur. Biophys. J. 39 (2010) 513–525.

[47] J. Belayi, M. Pas, P. Raspor, M. Pesti, T. Páli, Effect of hexavalent chromium on eukaryotic plasma membrane studied by EPR spectroscopy, Biochim. Biophys. Acta 1421 (1999) 175–182.

[48] E. Virág, J. Belayi, Z. Gazdag, C. Vágvölgyi, M. Pesti, Direct in vivo interaction of the antibiotic primycin with the plasma membrane of *Candida albicans*: an EPR study, Biochim. Biophys. Acta 1818 (2012) 42–48.

[49] E. Virág, J. Belayi, S. Kocsubé, C. Vágvölgyi, M. Pesti, Antifungal activity of the primycin complex and its main components A1, A2 and C1 on a *Candida albicans* clinical isolate, and their effects on the dynamic plasma membrane changes, J. Antibiot. 66 (2013) 67–72.

[50] R.-K. Li, J.E. Cutler, A cell surface/plasma membrane antigen of *Candida albicans*, J. Gen. Microbiol. 137 (1991) 455–464.

[51] C.L.M. Sgherri, P. Salvateci, M. Menconi, A. Raschi, F. Navari-Izzo, Interaction between drought and elevated CO_2 in the response of Alfalfa plants to oxidative stress, J. Plant Physiol. 156 (2000) 360–366.

[52] F. Navari-Izzo, M.F. Quartacci, C. Pinzino, N. Rascio, C. Vazzana, C.L.M. Sgherri, Protein dynamics in thylakoids of the desiccation-tolerant plant *Boea hygroscopica* during dehydration and rehydration, Plant Physiol. 124 (2000) 1427–1436.

[53] D.E. Budil, S. Lee, S. Saxena, J.H. Freed, Nonlinear-least-squares analysis of slow-motion EPR spectra in one and two dimensions using a modified Levenberg–Marquardt algorithm, J. Magn. Reson. Ser. A 120 (1996) 155–189.

[54] J.H. Freed, Theory of slow tumbling ESR spectra for nitroxides, in: L.J. Berliner (Ed.), Spin Labeling: Theory and Applications, vol. 1, Academic Press, New York, 1976, pp. 53–132.

[55] D.J. Schneider, J.H. Freed, Calculating slow motional magnetic resonance spectra: a user's guide, in: L.J. Berliner, L.J. Reuben (Eds.), Biological Magnetic Resonance, Plenum, New York, 1989, pp. 1–76.

[56] E. Meirovitch, A. Nayeem, J.H. Freed, Analysis of protein–lipid interactions based on model simulations of electron spin resonance spectra, J. Phys. Chem. 88 (1984) 3454–3465.

[57] E. Meirovitch, J.H. Freed, Analysis of slow-motional electron spin resonance spectra in smectic phases in terms of molecular configuration, intramolecular interactions, and dynamics, J. Phys. Chem. 88 (1984) 4995–5004.

[58] M. Ge, J.H. Freed, Electron-spin resonance study of aggregation of gramicidin in dipalmitoylphosphatidylcholine bilayers and hydrophobic mismatch, Biophys. J. 76 (1999) 264–280.

[59] Z. Liang, J.H. Freed, An assessment of the applicability of multifrequency ESR to study the complex dynamics of biomolecules, J. Phys. Chem. B 103 (1999) 6384–6396.

[60] O.H. Griffith, P.J. Dehlinger, S.P. Van, Shape of the hydrophobic barrier of phospholipid bilayers (evidence for water penetration into biological membranes), J. Membr. Biol. 15 (1974) 159–192.

[61] W.K. Subczynski, A. Wisniewska, J.J. Yin, J.S. Hide, A. Kusumi, Hydrophobic barriers of lipid bilayer membranes formed by reduction of water penetration by alkyl chain unsaturation and cholesterol, Biochemistry 33 (1994) 7670–7681.

[62] D. Marsh, Polarity and permeation profiles in lipid membranes, Proc. Natl. Acad. Sci. U. S. A. 98 (2001) 7777–7782.
[63] M. Ge, A. Gidwani, H.A. Brown, D. Holowka, B. Baird, J.H. Freed, Ordered and disordered phases coexist in plasma membrane vesicles of RBL-2H3 mast cells. An ESR study, Biophys. J. 85 (2003) 1278–1288.
[64] M.J. Swamy, L. Ciani, M. Ge, A.K. Smith, D. Holowka, B. Baird, J.H. Freed, Coexisting domains in the plasma membranes of live cells characterized by spin-label ESR spectroscopy, Biophys. J. 90 (2006) 4452–4465.
[65] H.-J. Kaiser, D. Lingwood, I. Levental, J.L. Sampaio, L. Kalvadova, L. Rajendran, K. Simons, Order and lipid phases in model and plasma membranes, Proc. Natl. Acad. Sci. U. S. A. 106 (2009) 16645–16650.
[66] L. Calucci, C. Pinzino, M.F. Quartacci, F. Navari-Izzo, Copper excess reduces the fluidity of plasma membrane lipids of wheat roots: a spin probe EPR study, J. Phys. Chem. B 107 (2003) 12021–12028.
[67] I. Perissi, S. Ristori, S. Rossi, L. Dei, G. Martini, Electron spin resonance and differential scanning calorimetry as combined tools for the study of liposomes in the presence of long chain nitroxides, J. Phys. Chem. B 106 (2002) 10468–10473.
[68] F. Cicogna, C. Pinzino, S. Castellano, A. Porta, C. Forte, L. Calucci, Interaction of azole compounds with DOPC and DOPC/ergosterol bilayers by spin probe EPR spectroscopy: implications for antifungal activity, J. Phys. Chem. B 117 (2013) 11978–11987.
[69] C.A. Hitchcock, K. Barrett-Bee, N.J. Russell, The lipid composition of azole-sensitive and azole-resistant strains of *Candida albicans*, J. Gen. Microbiol. 132 (1986) 2421–2431.
[70] N. Mago, G.K. Khuller, Lipids of *Candida albicans*: subcellular distribution and biosynthesis, J. Gen. Microbiol. 136 (1990) 993–996.
[71] P. Mishra, J. Bolard, R. Prasad, Emerging role of lipids of *Candida albicans*, a pathogenic dimorphic yeast, Biochim. Biophys. Acta 1127 (1992) 1–14.
[72] J. Löffler, H. Einsele, H. Hebart, U. Schumacher, C. Hrastnik, G. Daum, Phospholipid and sterol analysis of plasma membranes of azole-resistant *Candida albicans* strains, FEMS Microbiol. Lett. 185 (2000) 59–63.
[73] M. Insenser, C. Nombela, G. Molero, C. Gil, Proteomic analysis of detergent-resistant membranes from *Candida albicans*, Proteomics 6 (2006) S74–S81.
[74] L. Wang, Y. Jia, R.J. Tang, Z. Xu, Y.B. Cao, X.M. Jia, Y.-Y. Jiang, Proteomic analysis of Rta2p-dependent raft association of detergent-resistant membranes in Candida albicans, PloS ONE 7 (2012) e37768.